NASA TECHNICAL NOTE

NASA TN D-6660

NASA TN D-6660

FRETTING WEAR IN TITANIUM, MONEL-400, AND COBALT — 25-PERCENT MOLYBDENUM USING SCANNING ELECTRON MICROSCOPY

by Robert C. Bill

Lewis Research Center and
U.S. Army Air Mobility R&D Laboratory
Cleveland, Ohio 44135

1. Report No. NASA TN D-6660	2. Government Accession No.	3. Recipient's Catalog No.
4. Title and Subtitle FRETTING WEAR IN TITANIUM, MONEL-400, AND COBALT - 25-PERCENT MOLYBDENUM USING SCANNING ELECTRON MICROSCOPY		5. Report Date February 1972
		6. Performing Organization Code
7. Author(s) Robert C. Bill		8. Performing Organization Report No. E-6623
		10. Work Unit No. 132-15
9. Performing Organization Name and Address NASA Lewis Research Center and U.S. Army Air Mobility R&D Laboratory Cleveland, Ohio 44135		11. Contract or Grant No.
		13. Type of Report and Period Covered Technical Note
12. Sponsoring Agency Name and Address National Aeronautics and Space Administration Washington, D.C. 20546		14. Sponsoring Agency Code

15. Supplementary Notes

16. Abstract

Damage scar volume measurements taken from like metal fretting pairs combined with scanning electron microscopy observations showed that three sequentially operating mechanisms result in the fretting of titanium, Monel-400, and cobalt - 25-percent molybdenum. Initially, adhesion and plastic deformation of the surface played an important role. This was followed after a few hundred cycles by a fatigue mechanism which produced spall-like pits in the damage scar. Finally, a combination of oxidation and abrasion by debris particles became most significant. Damage scar measurements made on several elemental metals after 6×10^5 fretting cycles suggested that the ratio of oxide hardness to metal hardness was a measure of the susceptibility of a metal to progressive damage by fretting.

17. Key Words (Suggested by Author(s))		18. Distribution Statement
Fretting Fretting fatigue Scanning electron microscopy	Abrasion Adhesion	Unclassified - unlimited

19. Security Classif. (of this report) Unclassified	20. Security Classif. (of this page) Unclassified	21. No. of Pages 35	22. Price* $3.00

FRETTING WEAR IN TITANIUM, MONEL-400, AND COBALT - 25-PERCENT MOLYBDENUM USING SCANNING ELECTRON MICROSCOPY

by Robert C. Bill

Lewis Research Center and

U. S. Army Air Mobility R&D Laboratory

SUMMARY

The progressive development of fretting damage with increasing number of fretting cycles was measured on 99.9-percent copper, titanium, Monel-400, and cobalt - 25-percent molybdenum specimens. Also, damage measurements were made on several high-purity elemental metals after 6×10^5 fretting cycles. All tests were run in air at room temperature, except for a series of tests run on a titanium specimen in a nitrogen (N_2) atmosphere. The fretting oscillations were held to a constant amplitude (peak to peak) of 7.5×10^{-6} meter (0.003 in.) and a frequency of 55.8±0.2 hertz. The contact force between the mating specimens was 1.47 newtons (150 g).

In addition to the progressive damage measurements, scanning electron microscopy photographs were made at various stages of fretting in titanium, Monel-400, and cobalt - 25-percent molybdenum. These observations were correlated with the damage measurements, enabling a sequence of mechanisms responsible for the fretting damage in these materials to be identified. Up to at least 100 cycles, an adhesion - junction growth - fracture mechanism was most significant. After 1000 cycles, the presence of spall-like surface pits suggested the operation of a subsurface fatigue mechanism. Between 10 000 and 100 000 cycles, the accumulation of oxidized debris suggested that the fretting damage was being caused by a combination of oxidation and abrasion by oxidized debris particles. This hypothesis was further supported by experiments conducted on a titanium specimen in a N_2 atmosphere. The rate of fretting damage was observed to decrease steadily in N_2, whereas the specimen tested in air showed an increase in the rate of damage after about 3×10^4 cycles.

The elemental metals tested were aluminum, titanium, iron, copper, nickel, beryllium, columbium, tungsten, molybdenum, and lead. These materials generally show that the fretting damage produced by 6×10^5 cycles increases with the ratio of oxide hardness. It is proposed that this ratio provides a measure of the effectiveness of the oxidized debris as an abrasive.

INTRODUCTION

Fretting is a particular type of wear process usually characterized by a low-amplitude vibratory sliding motion between two contacting surfaces. Amplitudes as small as 5 to 10 Å may be sufficient to initiate fretting damage (refs. 1 and 2). One of the significant characteristics that separate fretting from other types of wear appears to be the retention of wear debris in the contact region.

Such measurements as specimen weight loss, damage scar volume, and fretting frictional force have been used to describe fretting damage. The scanning electron microscope (SEM) provides a unique opportunity for observing the progress of fretting damage. Such advantages as depth of focus, range of magnification (from less than ×10 to more than ×10 000), ease of specimen preparation, and a sensitivity to the chemical composition of microscopic features of the specimen make it very attractive. Further information on the SEM may be found in reference 3.

The purpose of this study is to use the SEM in conjunction with damage scar volume measurements to provide evidence needed to identify the fretting mechanisms operating in titanium, Monel-400, and cobalt - 25-percent molybdenum at room temperature in air. Also, several elemental metals were subjected to fretting in an effort to determine whether the ratio of oxide hardness to metal hardness is a measure of a metal's resistance to fretting.

BACKGROUND

Among the parameters that affect the fretting process in a given material are the normal force between the two surfaces, the temperature, the humidity, the contact geometry, and the frequency and magnitude of the oscillations (refs. 2 and 4). The observations of Feng and Uhlig (ref. 5) on mild steel indicate that the severity of the fretting damage increases as load and amplitude increase; and the damage is observed to decrease as frequency, humidity, and temperature increase. They also observed that the damage is reduced in an inert atmosphere. A later review article of the fretting literature (ref. 6) shows general agreement with the findings of Feng and Uhlig, with some uncertainty about the effect of humidity. In one case it appeared that the fretting damage was a minimum near 50-percent relative humidity, and in another case a maximum was observed at about 30-percent relative humidity.

Fretting is encountered as a practical problem in many design situations. Some typical examples include the mating surfaces of press-fit parts, the interface between parts and fasteners, precision instrument bearings subjected to vibration, overrunning clutch assemblies, splines, and universal joints. In jet engines, fretting is a problem

in the wire friction dampers of compressor blades (ref. 7), in the joints between the disks and the blades of turbines and compressors, and in the piston ring that comprises the secondary seal of the mainshaft seal assembly.

Considerable attention has been given to the effect that fretting might have on the fatigue strength of structural parts. Using the scanning electron microscope, Waterhouse and Taylor (ref. 8) have observed the initiation of fatigue cracks in the fretting region of 0.7-percent carbon steel specimens. Nishioka and Hirakawa (ref. 9) subjected specimens of various steels to simultaneous fatigue and fretting action. They attribute the formation of the fatigue cracks in these specimens to the combined stress state associated with the normal contact force and to the frictional force produced by the fretting motion. Direct measurements of fatigue life under conditions which fretting occurs (refs. 10 and 11) show that the fretting action definitely reduces the fatigue life. Thus, the possible occurrence of fretting should be considered in structural designs that are subjected to fatigue.

The details of the mechanisms of fretting are not well understood. Work by Godfrey, Bisson, and Bailey (refs. 12 to 14) demonstrates that adhesion is responsible for the initial stages of fretting damage, while corrosive effects play a secondary role in the fretting process. More recent investigations (refs. 15 and 16) support the findings of Godfrey, with the qualification that the generation of wear debris becomes important in the later stages of fretting. In an extensive review article, Hurricks (ref. 17) divides the process into three stages: (1) initial adhesion; (2) the generation of oxidized debris; and (3) steady-state wear probably caused by a fatigue mechanism. He further discusses the mechanism of the generation of oxide debris and points out a possible connection between the corrosion process and crack sites.

APPARATUS

A schematic diagram of the fretting apparatus is shown in figure 1. The oscillatory motion is provided by an electrically driven linear vibrator, much like the driver of a radio speaker. The motion is transmitted directly to the lower specimen by a rigid shaft leading through the bellows into the test chamber.

The amplitude (peak to peak) of the oscillations was monitored by a capacitance probe and was directly displayed as a deflection on a meter. Control of the amplitude was effected by controlling the rms voltage to the vibrator.

The frequency of oscillation was also monitored by the capacitance probe and was displayed on a digital counter as cycles per second. A variable oscillator was used to control the frequency of the signal to the vibrator and thus control the frequency of the fretting motion.

The load was applied to the specimen by placing precision weights into the load pan, which was hung from the load arm. The load arm, having a 3:1 mechanical advantage, transmitted the load through the bellows seal in the top of the apparatus to the specimen contact point. The beam could be conveniently positioned initially by means of the counterweight. A dial gage (not shown) at the top of the apparatus indicated the relative deflection of the top face of the bellows seal. This was used as a reference during the actual loading procedure.

When a controlled atmosphere was desired, the test chamber was sealed and a selected gas was bled through. A pressure gage (not shown), mounted at the top of the apparatus, monitored the internal positive pressure. The pressure was controlled by a valve mounted downstream from the gage.

MATERIALS

Titanium, Monel-400, and cobalt - 25-percent molybdenum were chosen for the study for two experimental reasons. The first is that the fretting scar surfaces may be readily cleaned, in an ultrasonic cleaner, of grosser deposits of debris after testing. This is a necessary characteristic if the SEM study is to reveal anything more than a featureless smear of debris. The second reason is that the volume of the fretting scars produced on these materials is reproducible and representative of the range of fretting damage observed in alloys and elemental metals. Copper, included in the progressive damage measurements, was not included in the SEM study because the oxidized debris required a hard scrub with an abrasive for its removal. It was felt that such a process would erase the finer detail of the fretting scar.

The titanium specimens were of 99.9 percent purity, as were the elemental metals used in this study. The nominal composition of the Monel-400 alloy is given in table I. The cobalt - 25-weight-percent molybdenum alloy has a hexagonal close-packed (hcp) structure and has been observed to show low coefficients of adhesion and friction (refs. 18 and 19).

SPECIMEN PREPARATION

The specimens were bullet shaped, 1.9 centimeters (3/4 in.) long, and 0.95 centimeter (3/8 in.) in diameter. One end was machine ground to a 0.48-centimeter (3/16-in.) spherical radius, and the other end was machined flat. The flat end was lapped after fabrication. In an experiment, the round end of one specimen (comprising the upper, stationary surface) was contacted against the flat end of a mating specimen (comprising the lower, moving surface).

Before running an experiment, the contacting surfaces of the mating specimens were scrubbed with levigated alumina, then rinsed with alcohol followed by a water rinse. A check was made of the water wettability of the specimen surface to assure that all oil films had been removed. In the case of the specimens that were examined in the SEM, the lapped flat surface was rubbed down on 4/0 grit emery paper, then mechanically polished using a 0.05-micrometer alumina polishing compound. Following the polish and rinse, the specimen was ultrasonically cleaned to assure the removal of the polishing alumina. The purpose of the polishing procedure was to provide a good background surface against which to contrast the fretting scar.

PROCEDURE

Running of Fretting Experiments

For experiments that were run in room air, the flange seal shown in figure 1 was removed from the chamber. The temperature of room air was 23° C $\pm 1^{\circ}$ C, and the relative humidity was 50 percent $\pm$ 10 percent. Experiments performed on mild steel by Feng and Uhlig (ref. 5) suggested that the humidity variation in this range would have a negligible effect on the experimental results.

In the case of experiments run in a flowing inert atmosphere, nitrogen was fed into the sealed test chamber. A positive pressure of 14 to 21 N/m^2 gage (1 to $1\frac{1}{2}$ psig) was maintained in the chamber. A constant flow rate of 0.7 to 1.0 cubic meter per hour (20 to 30 ft^3/hr) was run through the system; and the entire system was allowed to purge for 1/2 hour after sealing, prior to testing.

Before applying the load to the specimens, it was necessary to locate the deflection at which specimen-to-specimen contact occurred. This was easily done by manually deflecting the load arm, which deflected the bellows downward, until the vibration due to the oscillatory motion transmitted across the specimen-to-specimen interface could be felt. The dial indicator was then adjusted to read zero with the arm in this position, and the arm was released. Deadweights were then loaded onto the weight pan attached to the arm until the dial indicator again read zero, showing that the two surfaces were just contacting. There was sufficient hysteresis in the springs and bellows to enable the load system to be backed away from actual specimen contact until the controlled normal load between the two specimens was applied. For the tests in this study, this normal load was 50 grams as measured in the pan, or 1.47 newtons (150 g) at the specimen-specimen interface.

The other two parameters that were controlled to completely define the set of conditions under which a fretting experiment was run were the frequency and amplitude of

the oscillations. The frequency was controlled to 55.8 hertz ± 0.2 hertz, and the amplitude was held to 75×10^{-6} meter (0.003 in.) peak to peak.

Examination of Specimens

All specimens were given an ultrasonic cleaning after fretting to remove the loose debris that would otherwise obscure the details of the fretting scar and make measurements of the scar very difficult.

The wear volume of the flat-surface fretting scars was measured by using a light section microscope. By this technique, a plane beam of light is directed obliquely (45° angle of incidence) at the specimen surface. The reflected light beam is viewed through an optical microscope and appears as a straight horizontal line. Surface contours appear as deviations from this straight line. This method of examination is analogous to viewing a 45° taper section of the surface. A typical exposure taken through the light section microscope is shown in figure 2. Curved surfaces could be viewed as well as flat surfaces, but taking measurements from exposures of curved surfaces is extremely difficult and unreliable. For this reason, wear measurements were made on the flat surface.

It was assumed that the wear scars on the flat specimens were approximately in the shape of the cap of a sphere. The volume V of these wear scars was then calculated by using the formula

$$V = 0.1 \times d^2 \times 4h$$

where d is the wear scar diameter and h is the maximum depth of the scar. The measured quantities d and h are shown schematically in figure 3.

By using secondary electron imaging, wear spots were examined at various levels of magnification in the SEM. A low-magnification exposure (usually ×300) allowed an overview of the entire fretting scar. At ×900 or ×1500 a detailed view of a significant portion of the scar could be made. One or two exposures were taken at ×3000 to reveal any interesting features observed in the lower magnification exposures.

RESULTS AND DISCUSSION

The volume of the damage scars as a function of the cumulative number of fretting cycles is shown in figure 4. Initially, all specimens show a high rate of increase in wear volume. This rate declines with increasing number of cycles, possibly because

the general stress level decreases as the contact area increases. In the case of copper and titanium in air, an increased rate of damage is observed at fretting cycles greater than 10^4. Notice that the titanium specimen tested in N_2 showed no increased rate of damage. This suggests that oxidation may be playing an important role in the later stages of the fretting tests on titanium and copper.

The results of the SEM study provide further detailed information concerning the fretting mechanisms for titanium, Monel-400, and cobalt - 25-percent molybdenum. Before further discussion, it would be helpful to consider some general features observed in the SEM micrographs, examples of which are shown in figure 5.

The features labeled A in figure 5(a) have a "taffy" appearance, suggesting that the material had undergone severe plastic deformation followed by fracture. The formation of such features is good evidence that adhesion between the two surfaces occurred and led to junction growth and fracture. This sequence of events is discussed by Bowden and Tabor (ref. 20), and plastic deformation following adhesion has been directly observed using field ion microscopy techniques (ref. 21).

The region labeled B in figure 5(a) is composed of builtup material, protruding above the surrounding surface of the specimen. This material must have been extruded from the central portion of the damage scar.

Figure 5(b) shows many examples of what will be called "spall-like" pits. In figure 5(c), a higher magnification exposure of the region shown in the box in figure 5(b), can be seen the presence of serrations, denoted by "S," at the bottom of one of the spall-like pits. It is suggested that such serrations indicate the progressive growth of a low-cycle-fatigue crack.

The features cited in figure 5 are typical of those observed in titanium and Monel-400 after various numbers of fretting cycles. In the case of cobalt - 25-percent molybdenum, the features are somewhat different, but their interpretation is more straightforward, as will be seen.

Titanium

After 100 fretting cycles, the scars produced on titanium in air (fig. 6) are little different from those produced in N_2 (fig. 7). At this stage, the fretting scars are similar to unidirectional sliding wear scars but are somewhat rougher. This roughness is no doubt due to the reversed motion of the fretting action, but the basic mechanisms operating are probably adhesion - junction growth - fracture of junctions. Also, material buildup around the edges of the scar in figure 6 suggests the action of an extrusion process on a fine scale.

After 1000 fretting cycles in N_2 (fig. 8), numerous spall-like features, cited in the discussion of figure 5, appear on titanium. The bottom of one of these pits, which

happened to be very free of debris, reveals the serrated structure, suggesting the progressive development of a subsurface fatigue crack. There is not so much evidence for the continued action of the adhesion-initiated sequence of events, which operated at least up to 100 cycles. This could be due to the extreme strain hardening of the surface of the specimen in the vicinity of the wear scar. Such strain hardening would reduce the amount of plastic deformation to fracture following an adhesion event. Hence, there would be less junction growth associated with adhesion, reducing the amount of surface disruption produced by the adhesion mechanism.

Figure 9 shows the fretting scar produced on titanium by 1000 cycles run in air. The most significant feature that distinguishes this scar from the one in figure 8 (nitrogen environment) is the presence of particulate debris on the surface. This debris is particularly dense in the pits where it seems to collect. The appearance of the edges of the pits suggests a "leafy" or layered structure. It looks as though this leafy structure disintegrates during fretting, possibly through a corrosion fatigue cracking process (ref. 22), producing much of the debris observed. The concentration of the debris around the edges of the pit and the ragged appearance of the edges lend support to the disintegration hypothesis.

The scar produced by 10 000 cycles in N_2 (fig. 10) is essentially the same as the one resulting from 1000 cycles in N_2 (fig. 7). Similar spall-like pits are present, and the surrounding surface regions are fairly smooth.

Similarly, the scar produced by 10 000 cycles in air (fig. 11) differs only in size and detail from the one shown in figure 9 (1000 cycles in air). There appears to be more debris in the pits, and the leafy structure shows further evidence of disintegration.

Examination of titanium specimens run in air for 10^5 cycles (fig. 12) again reveals the large pits, but the surface features in the regions outside the pits seem to be obscured. This could be due to a buildup of compacted oxide debris in the contact region (as suggested by the dark patches in fig. 12) or to an abrasive action by the oxidized debris particles.

Monel-400

The Monel-400 specimens were tested at room temperature in air only.

After 100 cycles, Monel-400 (fig. 13) showed evidence that the adhesion - junction growth - fracture mechanism suggested for titanium is active. Of particular interest is the prominent particle in the center of the damage scar shown in figures 13(a) and (b). This particle may have been either transferred from the mating bullet or plucked out of the flat surface and bent back, hinge like, to its observed position. In any case it appears to be firmly adhering to the flat surface at its upper edge. Another significant feature is the spall-like pit with a serrated bottom visible in figure 13(c). From

this feature, it appears that a low-cycle-fatigue mechanism has already begun in Monel-400 after 100 cycles. Also notice the extruded metal at the bottom of the fretting scar (fig. 13(a)).

Figure 14 shows the surface of the Monel specimen after it was subjected to 1000 fretting cycles. The general features are similar to those of the scar produced by 100 cycles. The large fragment (fig. 14(a)), as wide as the fretting scar, shows strong evidence of having been transferred from the mating spherical surface. The roughened features on the upper surface of the fragment, and similar features on the wear scar just above the fragment, are typical of the elongated dimples produced in ductile fracture.

There is considerable particulate debris present around the edges of the fretting scar on Monel after 10 000 cycles (fig. 15). This debris buildup, coinciding roughly with the onset of accelerated wear, may mark the onset of the operation of an oxide particle abrasion mechanism.

Figures 16 and 17 show the fretting scars produced on Monel by 5×10^4 and 10^5 cycles, respectively. The fine crack network and surface disintegration indicate a simultaneous surface oxidation and fatigue action. The crack network is typical of the surface features produced as a material oxidizes, when the surface oxide film has a smaller specific volume than the bulk material; this puts the oxide film in tension and generally results in cracking. In addition to the crack network, the remnants of disintegrating spall pit edges may be seen. These features are similar to those observed in titanium after 1000 or 10 000 cycles. Thus, there is some evidence that the debris generation in the latter portion of the fretting process of Monel may come about from both a fatigue corrosion cracking of the surface pit edges and a direct surface oxidation mechanism.

Cobalt - 25-Percent Molybdenum

The SEM photographs of the cobalt - 25-percent molybdenum specimens fretted in air are somewhat different from those of the titanium and Monel-400 specimens. From 100 cycles to 3×10^4 cycles (figs. 18 to 20) the dominant feature of the fretting scars is the presence of fine scratches in the central region of the scars, with the accumulation of debris (indicated in fig. 18) around these scratches. There is little evidence for the action of a strong adhesion mechanism in the initial stages of fretting in cobalt - 25-percent molybdenum. Perhaps this is the key to the small amount of fretting damage observed on this material.

After 2×10^5 cycles (fig. 21) the scratches have nearly vanished, and some dark oxide debris may be seen at the edges of the damage scar (fig. 21(a)). The surface

gives the impression of having been polished by the oxidized debris. In fact, the phase distribution can be seen in the high-magnification exposures, with the molybdenum-rich phase appearing light.

Elemental Metal Study

So far, the results of this fretting study indicate that beyond about 10 000 cycles, the fretting damage mechanism is associated with oxidation and possibly abrasion by the oxidized debris. Certainly, the adhesion and early fatigue processes developed a surface condition that was either conducive to oxidation (as in Ti and Monel) or resistant to it (as in a Co-25Mo). Therefore, it seemed reasonable to examine the fretting damage in several elemental metals having a range of oxide- to metal-hardness ratios. Presumably the higher the ratio, the more abrasive the oxide would be to the metal. This hypothesis was considered by Hurricks (ref. 17) but was not given a strong endorsement, and Rabinowicz (ref. 23) has suggested that metals producing soft oxides have a self-lubricating capacity in sliding friction tests.

To check this hypothesis, specimens of aluminum, titanium, iron, copper, nickel, beryllium, columbium, tungsten, molybdenum, and lead were subjected to a single exposure period of 6×10^5 fretting cycles in air. In figure 22, the volume of the fretting scars is measured as a function of the ratio of oxide hardness to metal hardness for each elemental metal tested. The values of the ratio of oxide hardness to metal hardness were taken from reference 17. In every case, the oxide hardness is that of the higher oxide of the metal, and the metal hardness refers to the annealed state.

With a few exceptions (tungsten and beryllium), the trend seems to be one of increased fretting damage with increased ratio of oxide hardness to metal hardness. In the case of beryllium and tungsten, very little debris was observed; the real ratio of debris hardness to metal hardness may therefore be close to 1. For purposes of comparison, a high graphitic carbon and a low graphitic carbon are included. Their results lie close to the expected value for a metal with a 1:1 oxide- to metal-hardness ratio. This should not be surprising, as carbon produces no solid oxide debris and any debris present in the contact region would be solid carbon.

One must, of course, be cautious in drawing conclusions from figure 22. Oxidation rates are not considered, nor are the mechanical properties of the metal aside from the oxide- to metal-hardness ratio. It is an indication, though, that the abrasive aspect of fretting wear should be considered.

10

CONCLUSIONS

The combination of wear volume measurements and scanning electron microscope (SEM) observations of fretting in titanium, Monel-400, and cobalt - 25-percent molybdenum leads to the following conclusions:

1. Fretting occurs as a sequence of three mechanisms:

   Stage I: Fretting damage is initiated by an adhesion - junction growth - fracture process, much as in unidirectional sliding. This process dominates the first few hundred fretting cycles.

   Stage II: The cyclic stresses associated with the fretting motion lead to the development of a fatigue process which is clearly in evidence after 1000 cycles.

   Stage III: Fretting in air produces significant amounts of loose oxidized debris. The generation of this debris seems to be aided by a fatigue corrosion cracking process, as is made evident by the disintegration of material around the fatigue-associated surface pits. It seems that this debris can either enhance fretting damage through an abrasive action or mitigate it through a lubrication action. It is observed that this third stage is suppressed in titanium specimens fretted in a N_2 atmosphere.
   Notice that the order of the second and third stages is essentially reversed from that of the model proposed by Hurricks.

2. Cobalt - 25-percent molybdenum resists fretting damage far more than any of the other materials examined in this study. SEM observations give indications that this is due to the small development of adhesive and fatigue damage in the initial stages of fretting.

3. Experiments performed on elemental metals show a trend of increasing fretting damage as the ratio of oxide hardness to metal hardness increases. This is interpreted to mean that the abrasiveness of the oxide particles against the base metal is a significant parameter in evaluating the fretting resistance of a metal.

Lewis Research Center,
    National Aeronautics and Space Administration,
        and
U.S. Army Air Mobility R&D Laboratory,
    Cleveland, Ohio, November 12, 1971,
        132-15.

REFERENCES

1. Tomlinson, G. A.; Thorpe, P. L.; and Gough, H. J.: An Investigation of the Fretting Corrosion of Closely Fitting Surfaces. Proc. Inst. Mech. Eng., vol. 141, no. 3, May 1939, pp. 223-249.

2. Campbell, W. E.: Current Status of Fretting Corrosion. Symposium on Fretting Corrosion. Spec. Tech. Publ. No. 144, ASTM, 1953, pp. 3-23.

3. Thornton, P. R.: Scanning Electron Microscopy. Chapman & Hall, Ltd., 1968.

4. Bethune, B.; and Waterhouse, R. B.: Electrochemical Studies of Fretting Corrosion. Wear, vol. 12, 1968, pp. 27-34.

5. Feng, I-Ming; and Uhlig, Herbert H.: Fretting Corrosion of Mild Steel in Air and in Nitrogen. J. Appl. Mech., vol. 21, no. 4, Dec. 1954, pp. 395-400.

6. Anon.: Fretting and Fretting Corrosion. Lubrication, vol. 52, no. 4, 1966, pp. 49-64.

7. Swikert, Max A.; and Johnson, Robert L.: Friction and Wear Under Fretting Conditions of Materials for Use as Wire Friction Dampers of Compressor Blade Vibration. NASA TN D-4630, 1968.

8. Waterhouse, R. B.; and Taylor, D. E.: The Initiation of Fatigue Cracks in a 0.7% Carbon Steel by Fretting. Wear, vol. 17, no. 2, Feb. 1971, pp. 139-147.

9. Nishioka, Kunio; and Hirakawa, Kenji: Fundamental Investigations of Fretting Fatigue. Parts 3 and 4. Bull. JSME, vol. 12, no. 51, 1969, pp. 397-414.

10. Stepanov, V. N.: The Fatigue Diagram Features in Conditions of Fretting Corrosion. Fiz.-Khim. Mekh. Mater., vol. 3, no. 3, 1967, pp. 282-285.

11. Rimbey, Donald H.: An Experimental Study of Fretting Corrosion and Its Influence on Fatigue Strength. Ph.D. Thesis, Univ. Illinois, 1967.

12. Godfrey, Douglas: Investigation of Fretting by Microscopic Observation. NACA Rep. 1009, 1951.

13. Godfrey, D.; and Bisson, E. E.: NACA Studies of Mechanism of Fretting (Fretting Corrosion) and Principles of Mitigation. Lubr. Eng., vol. 8, no. 5, Oct. 1952, pp. 241-243, 262-263.

14. Godfrey, D.; and Bailey, J. M.: Early Stages of Fretting of Copper, Iron & Steel. Lubr. Eng., vol. 10, no. 3, May-June 1954, pp. 155-159.

15. Bethune, B.; and Waterhouse, R. B.: Adhesion of Metal Surfaces Under Fretting Conditions. I. Like Metals in Contact. Wear, vol. 12, 1968, pp. 289-296.

16. Halliday, J. S.: Experimental Investigation of Some Processes Involved in Fretting Corrosion. Proceedings of the Conference on Lubrication and Wear. Inst. Mech. Eng., Oct. 1-3, 1957, pp. 640-644.

17. Hurricks, P. L.: The Mechanism of Fretting - A Review. Wear, vol. 15, 1970, pp. 389-409.

18. Buckley, Donald H.; and Johnson, Robert L.: Marked Influence of Crystal Structure on the Friction and Wear Characteristics of Cobalt and Cobalt Base Alloys in Vacuum to 10^{-9} Millimeter of Mercury. II - Cobalt Alloys. NASA TN D-2524, 1964.

19. Johnson, Robert L.: Alloys as Bearing Materials for Total Hip Replacement. NASA TM X-52745, 1969.

20. Bowden, F. P.; and Tabor, D.: The Friction and Lubrication of Solids. Part II. Clarendon Press, Oxford, 1964, p. 72.

21. Brainard, William A.; and Buckley, Donald H.: Preliminary Study by Field Ion Microscopy of the Adhesion of Platinum and Gold to Tungsten and Iridium. NASA TN D-6492, 1971.

22. Meyn, D. A.: An Analysis of Frequency and Amplitude Effects on Corrosion Fatigue Crack Propagation in Ti-8Al-1Mo-1V. Metallurg. Trans., vol. 2, no. 3, Mar. 1971, pp. 853-865.

23. Rabinowicz, Ernest: Lubrication of Metal Surfaces by Oxide Film. ASLE Trans., vol. 10, no. 4, Oct. 1967, pp. 400-407.

TABLE I. - NOMINAL COMPOSITION

OF MONEL-400

Element	Composition of Monel-400, wt %
Ni	66
C	.3
Mn	2.00
Fe	2.50
S	.024
Si	.50
Cu	Balance
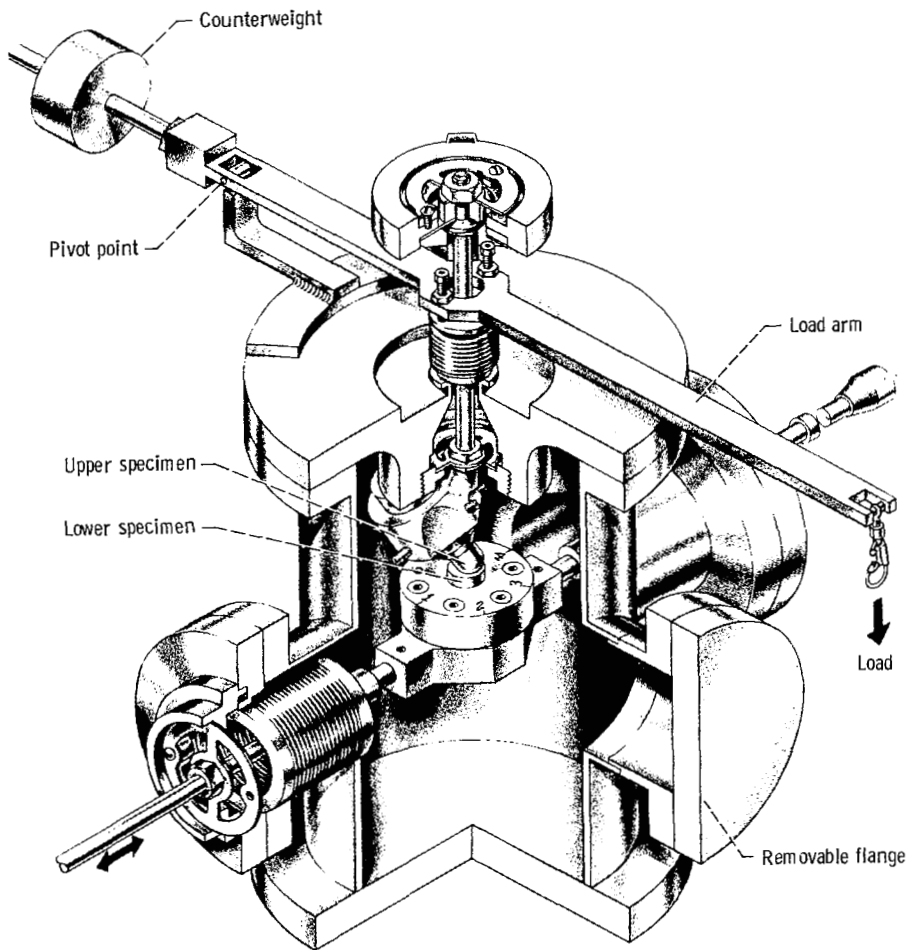
CD-11081-17

Figure 1. - Fretting apparatus.

14
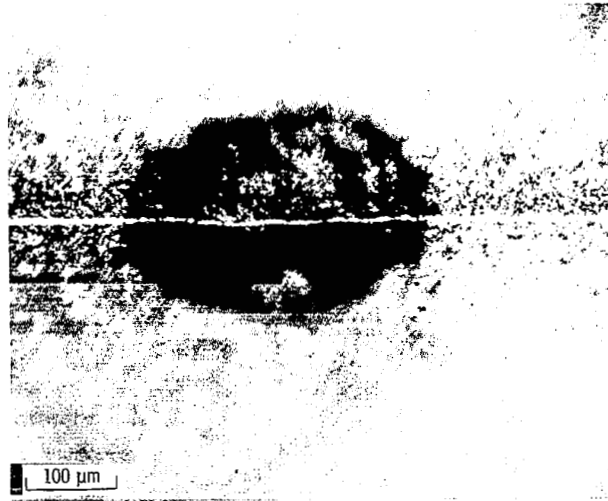
Figure 2. - Light section view of damage scar produced on titanium specimen after 10^5 fretting cycles against titanium in air. Relief magnification, 1.4 times as great as in-plane magnification.

Direction of oscillation

Typical scar shape after 10^2 to 10^3 cycles

Direction of oscillation

Typical scar shape after 10^4 or more cycles
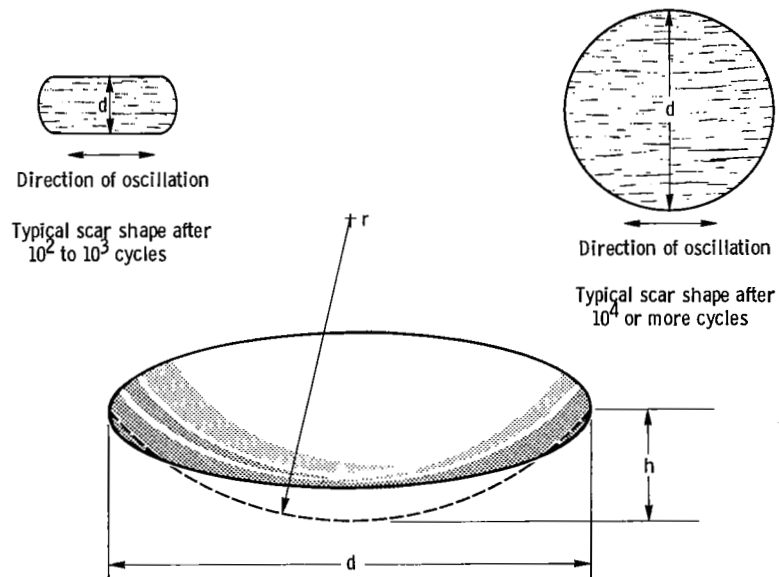
Figure 3. - Model of fretting wear scar, showing direction d across which light section measurements were made.
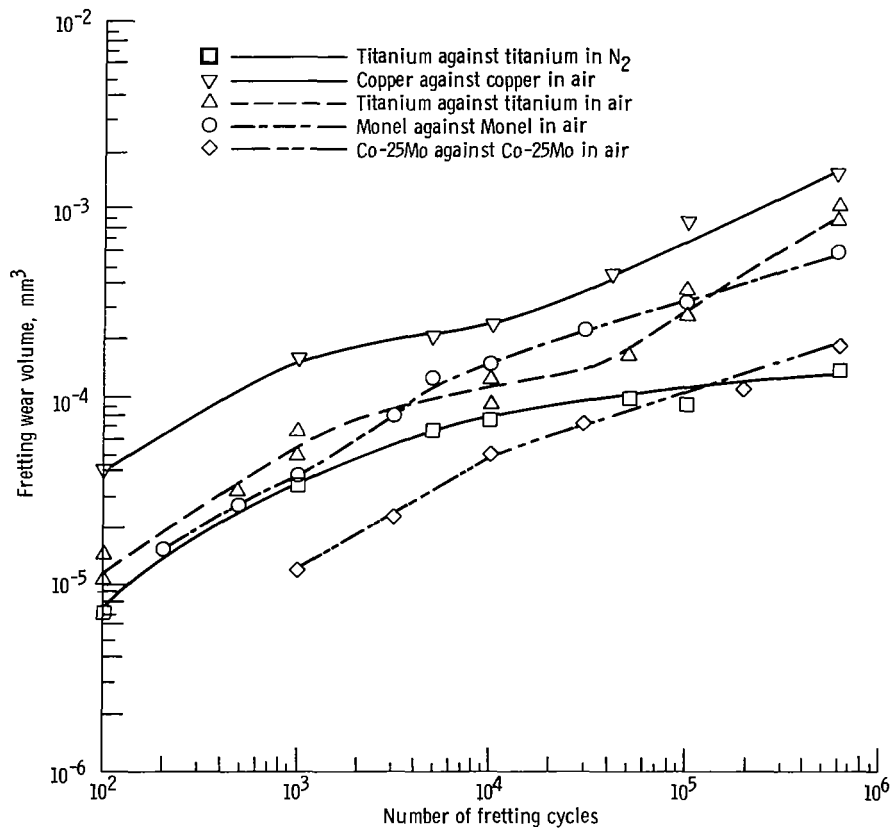
Figure 4. – Fretting wear volume as function of number of fretting cycles. Frequency, 55.8 hertz; normal force, 1.47 newtons (150 g); amplitude, 75×10^{-6} meter.
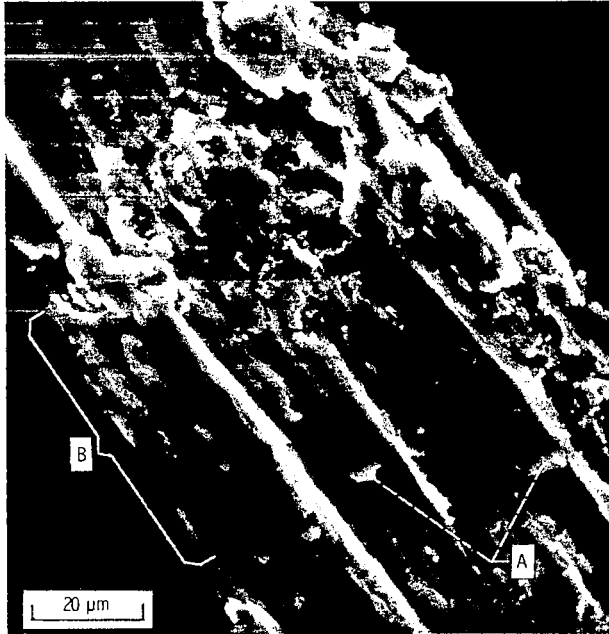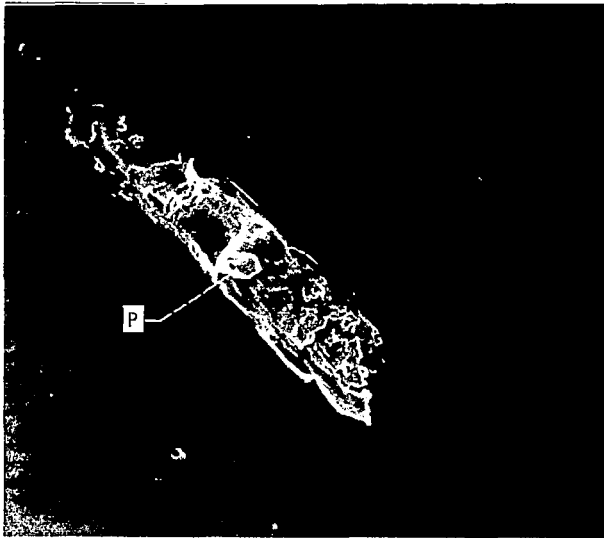
(a) Magnification, X900.
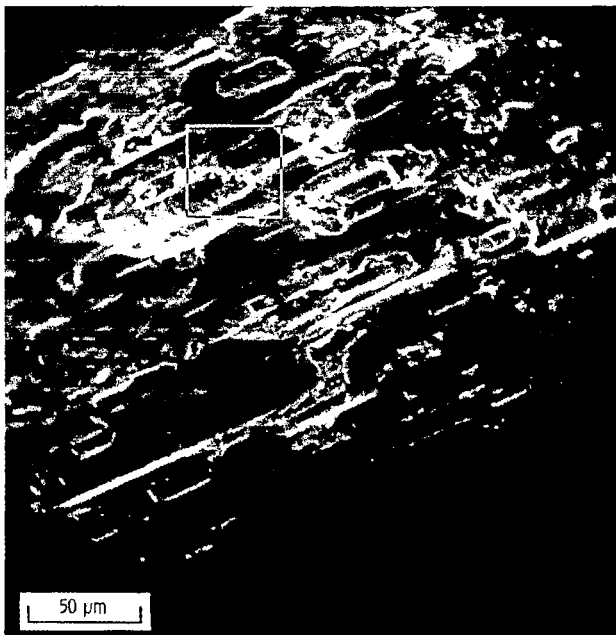
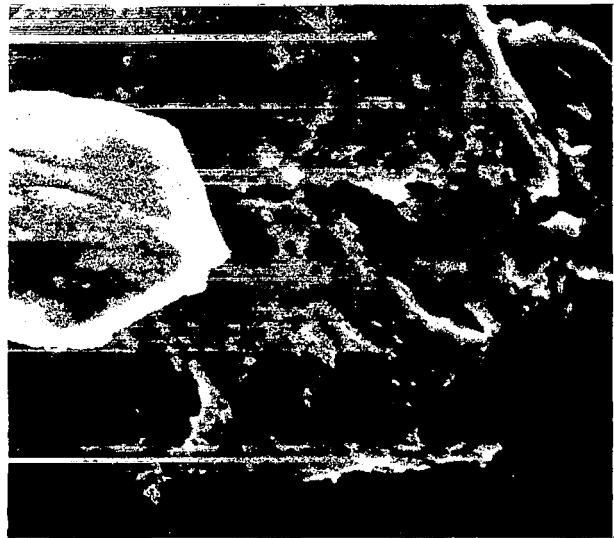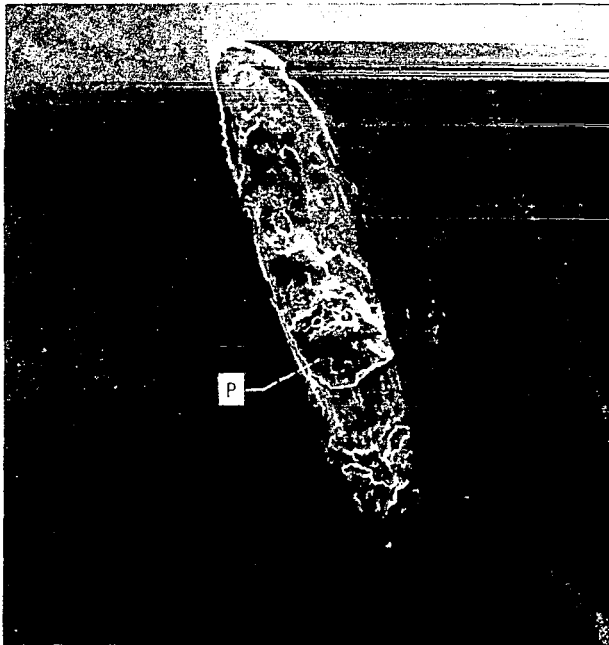(b) Magnification, X300.
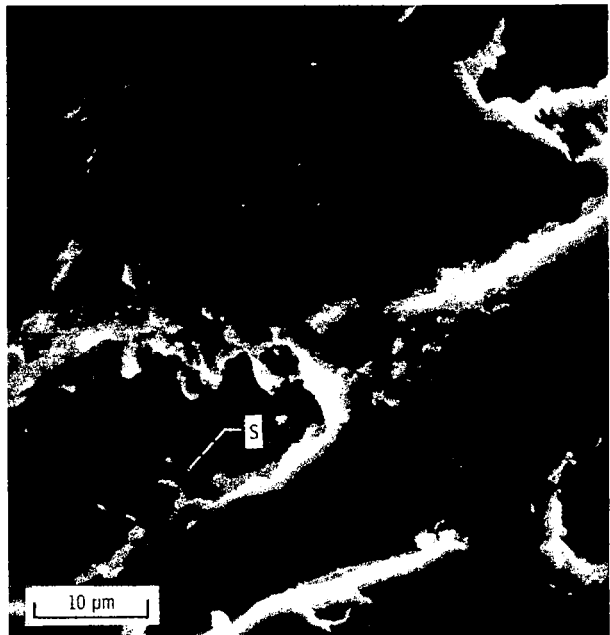
(c) Magnification, X1500.

Figure 5. - Scanning electron micrographs showing features generally observed in fretting scars of titanium and Monel-400.
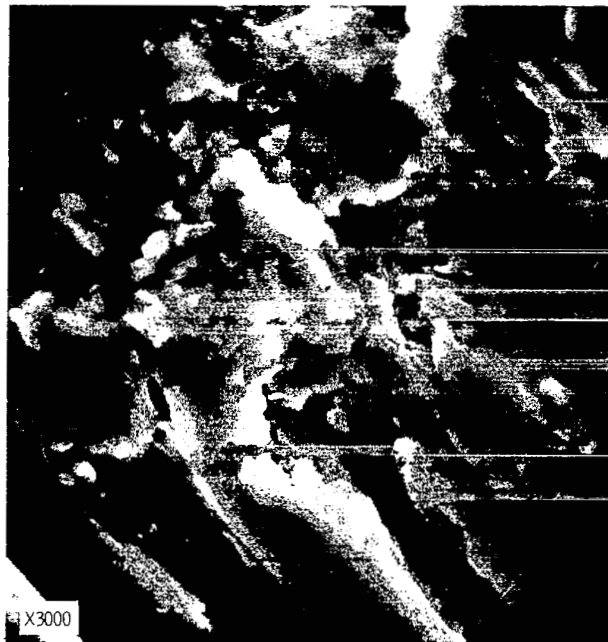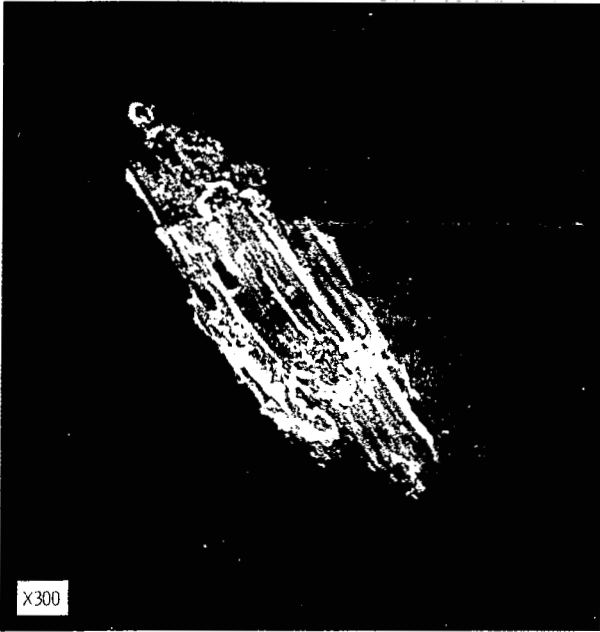
Figure 6. - Scanning electron micrographs of titanium fretted against titanium for 10^2 cycles in room-temperature air. Frequency, 55.8 hertz; normal force, 1.47 newtons (150 g); amplitude, 75×10^{-6} meter.
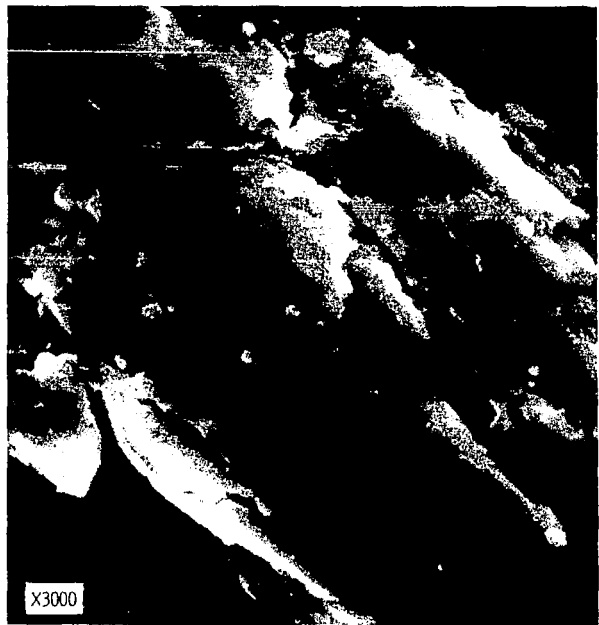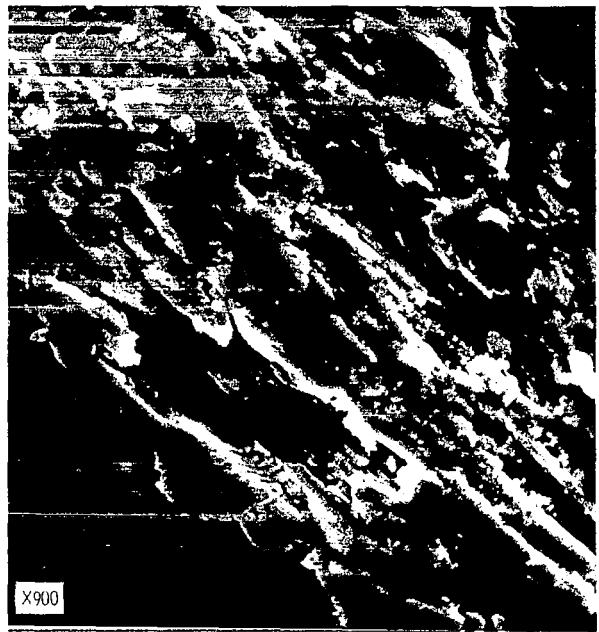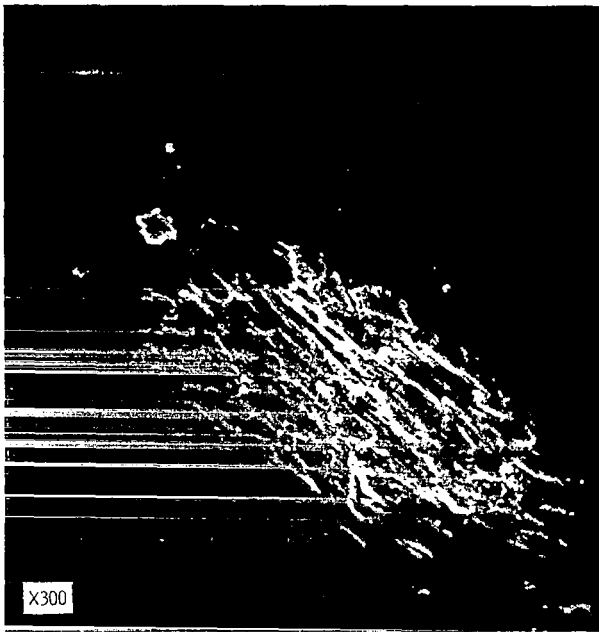
Figure 7. - Scanning electron micrographs of titanium fretted against titanium for 10^2 cycles in nitrogen at room temperature. Frequency, 55.8 hertz; normal force, 1.47 newtons (150 g); amplitude, 75×10^{-6} meter.
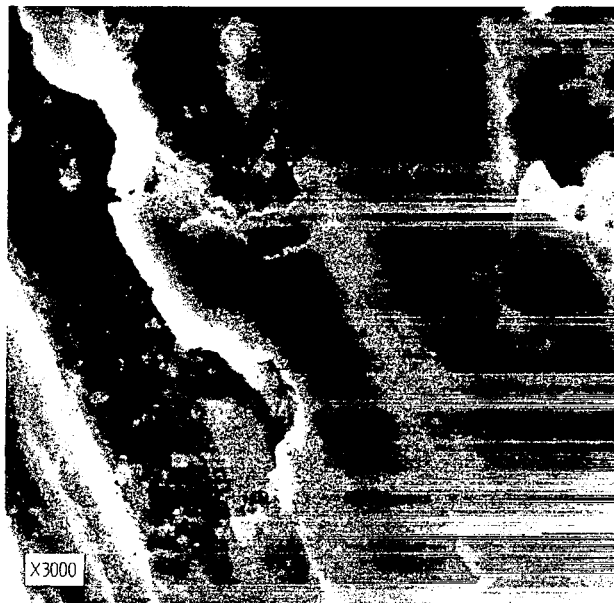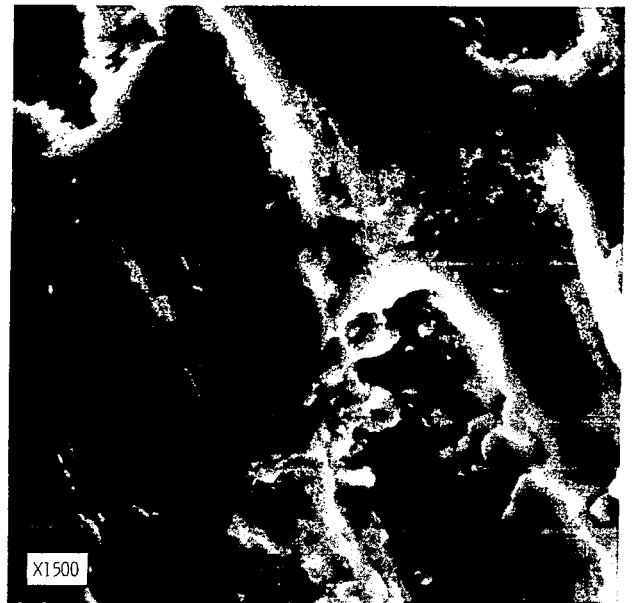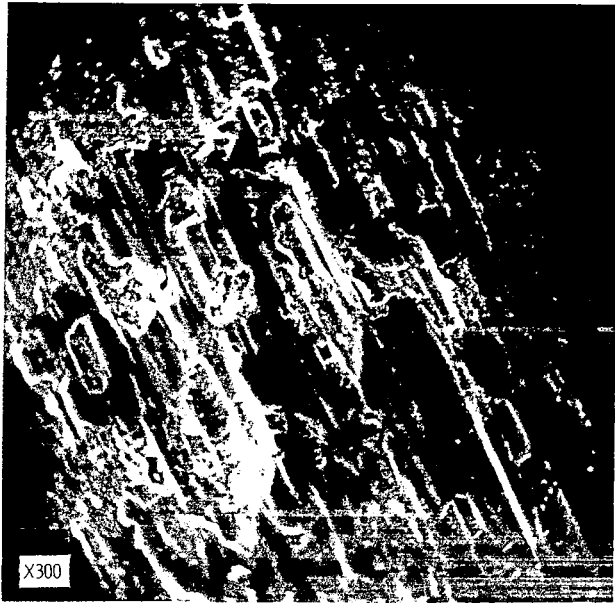
Figure 8. – Scanning electron micrographs of titanium fretted against titanium for 10^3 cycles in nitrogen at room temperature. Frequency, 55.8 hertz; normal force, 1.47 newtons (150 g); amplitude, 75×10^{-6} meter.
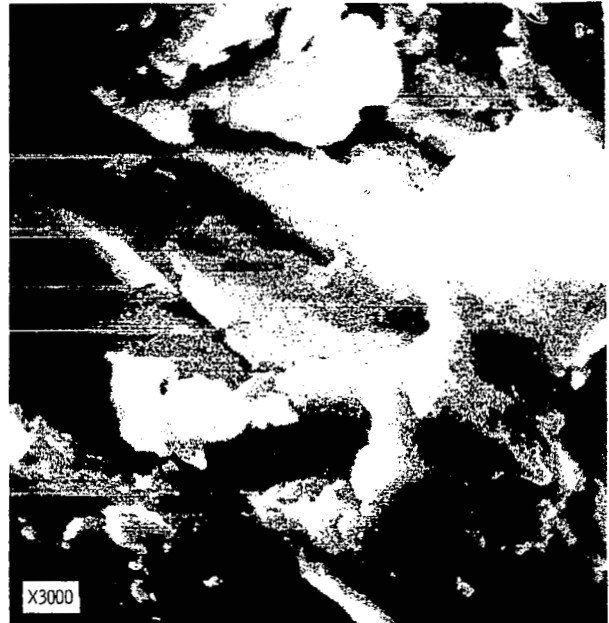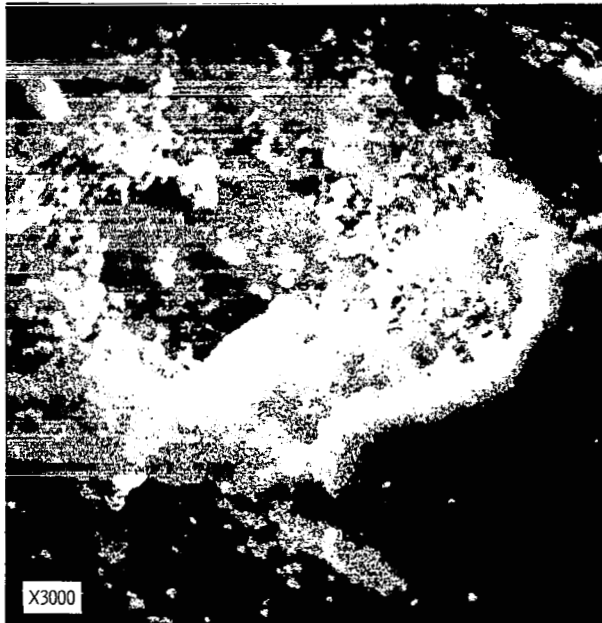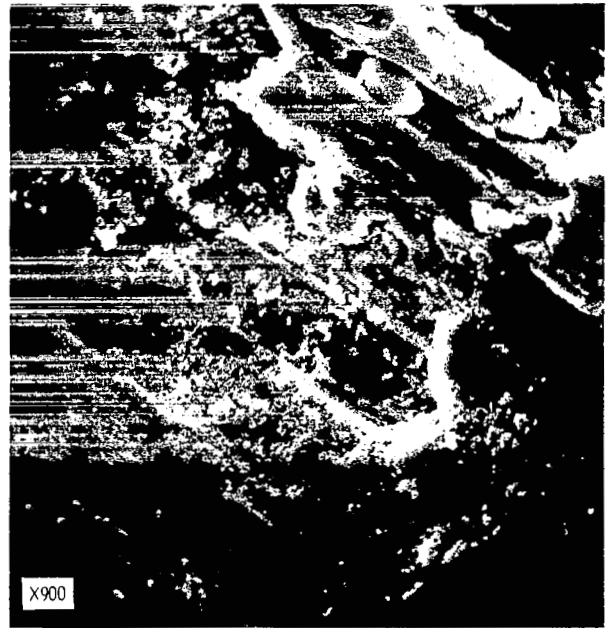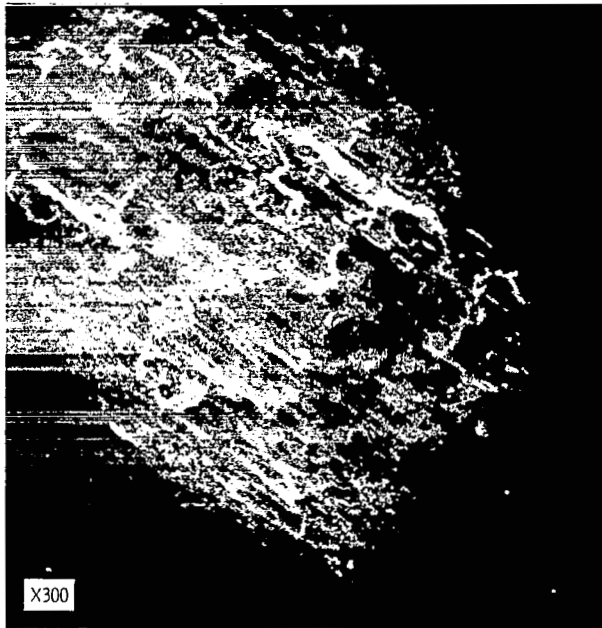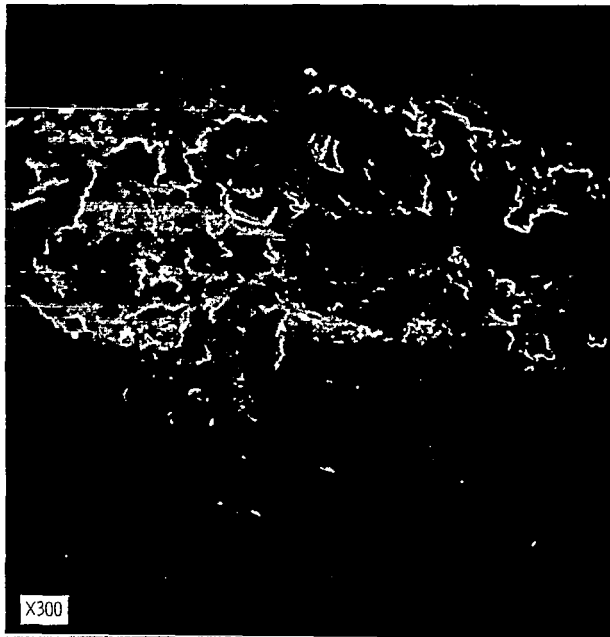
Figure 9. - Scanning electron micrographs of titanium fretted against titanium for 10^3 cycles in air at room temperature. Frequency, 55.8 hertz; normal force, 1.47 newtons (150 g); amplitude, 75×10^{-6} meter.

Figure 10. - Scanning electron micrographs of titanium fretted against titanium for 10^4 cycles in nitrogen at room temperature. Frequency, 55.8 hertz; normal force, 1.47 newtons (150 g); amplitude, 75×10^{-6} meter.
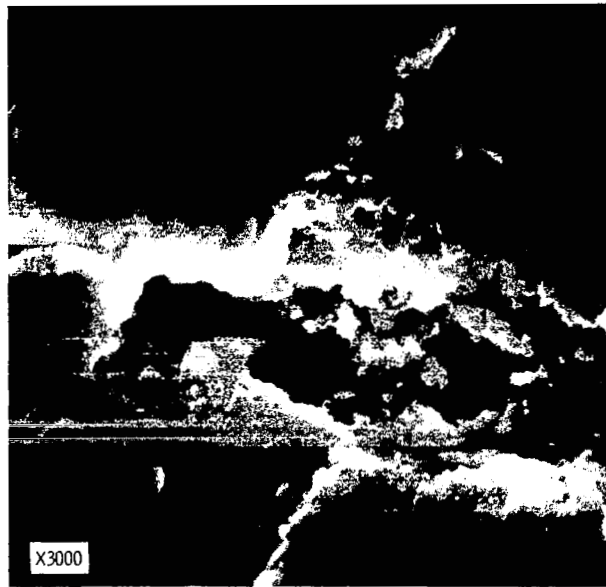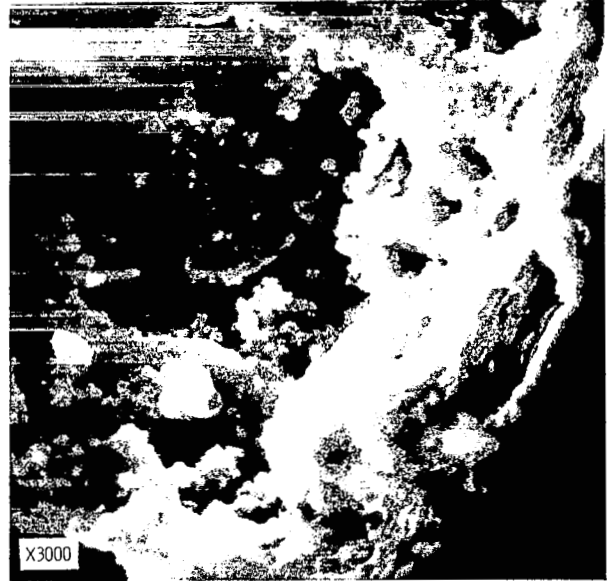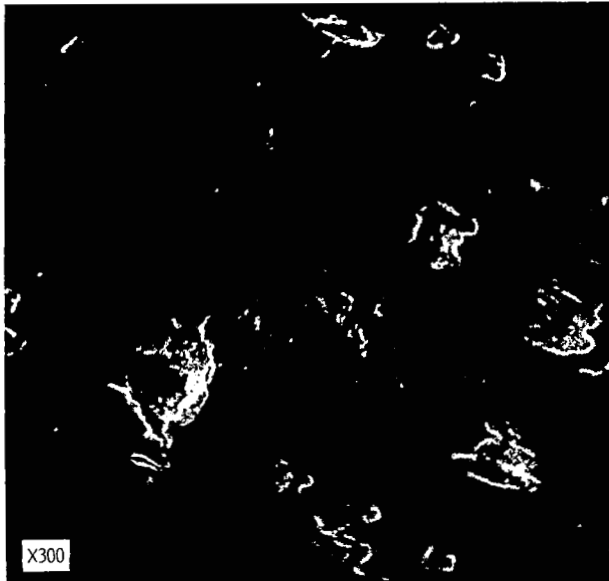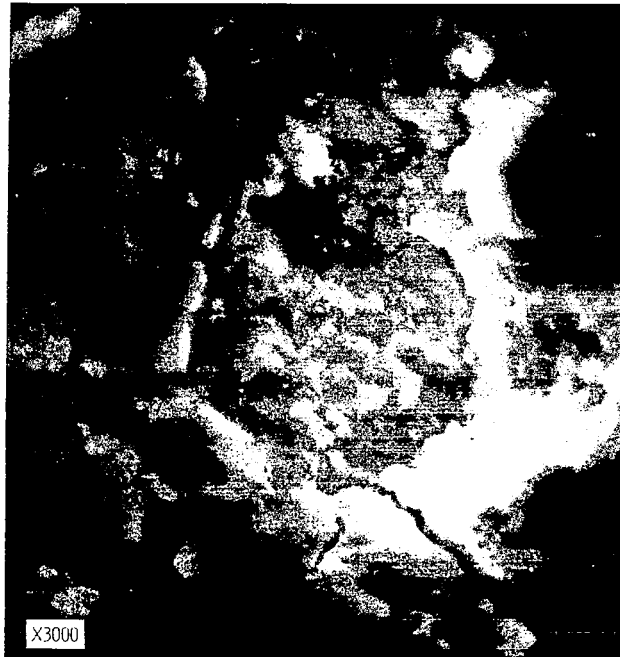
Figure 11. - Scanning electron micrographs of titanium fretted against titanium for 10^4 cycles in air at room temperature. Frequency, 55.8 hertz; normal force, 1.47 newtons (150 g); amplitude, 75×10^{-6} meter.
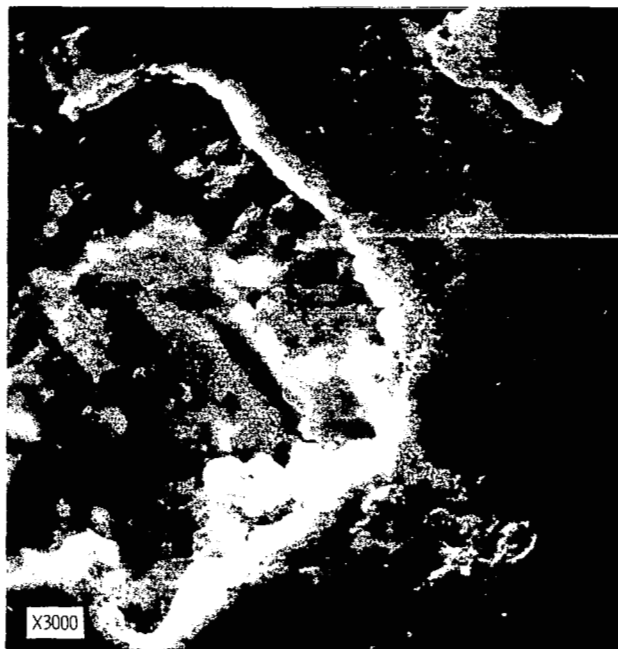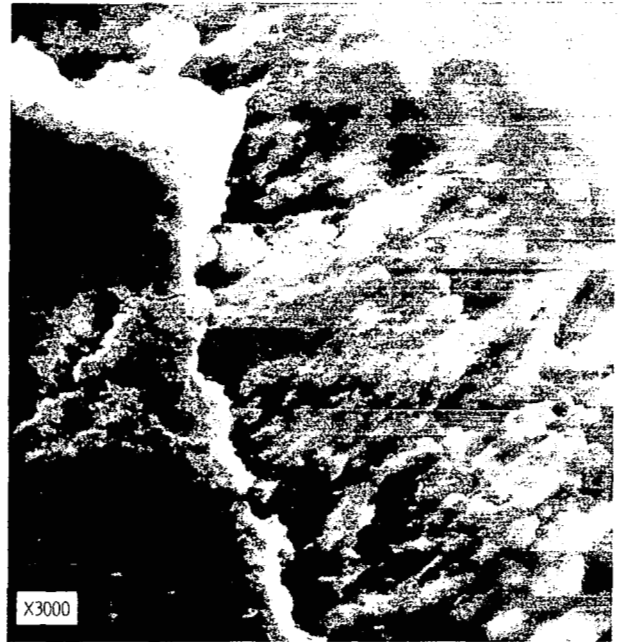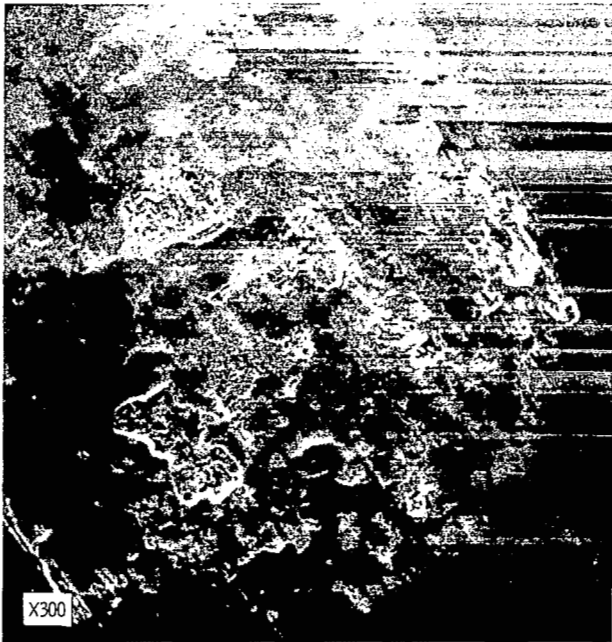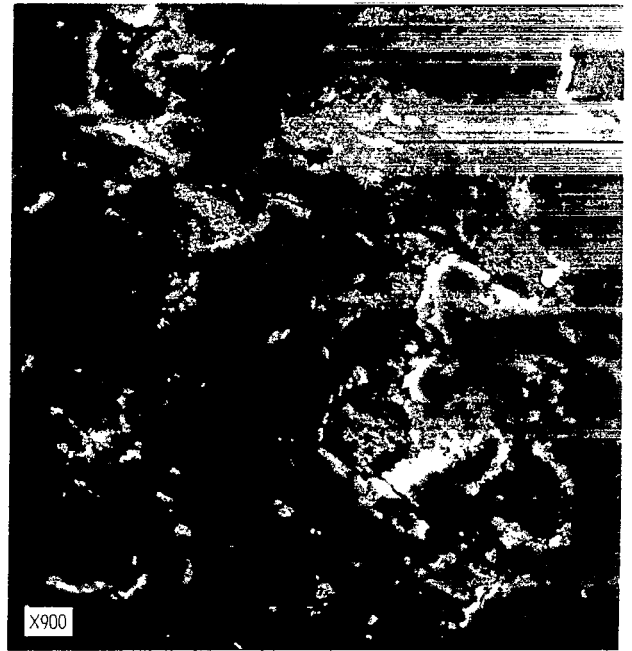
Figure 12. – Scanning electron micrographs of titanium fretted against titanium for 10^5 cycles in air at room temperature. Frequency, 55.8 hertz; normal force, 1.47 newtons (150 g); amplitude, 75×10^{-6} meter.

(a) Magnification, X300.
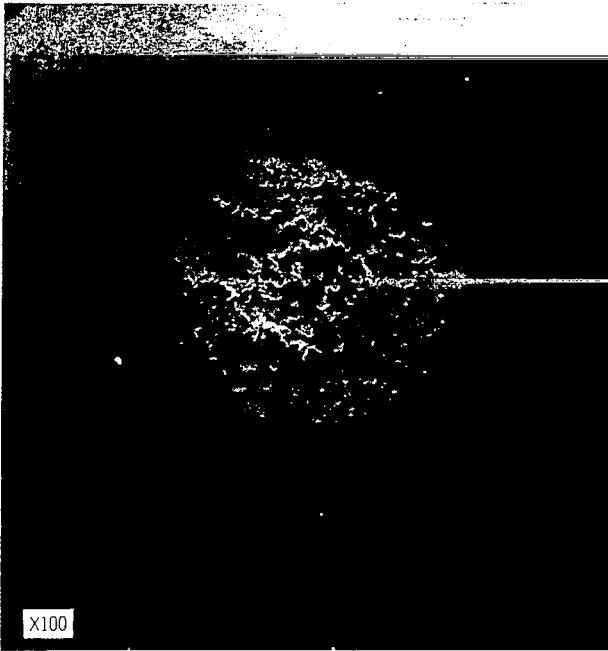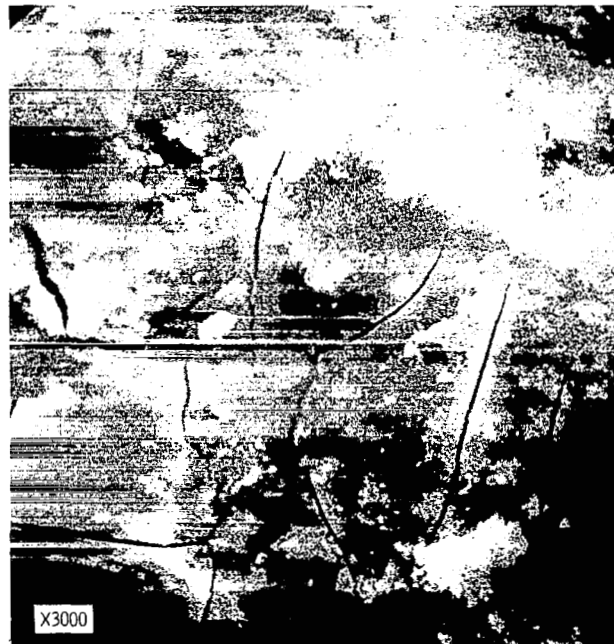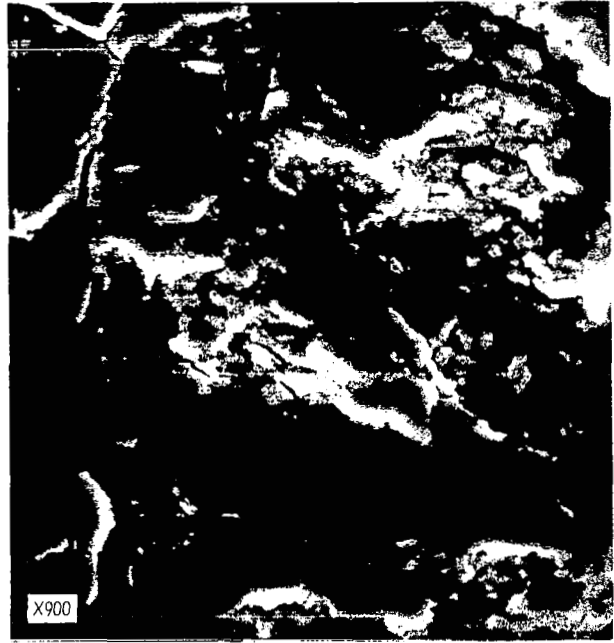
(b) Magnification, X900.

(c) Magnification, X3000.

Figure 13. – Scanning electron micrographs of Monel fretted against Monel for 10^2 cycles in air at room temperature. Frequency, 55.8 hertz; normal force, 1.47 newtons (150 g); amplitude, 75×10^{-6} meter. (Note transfer particle (P) in (a) and (b).)

(a) Magnification X300.

(b) Magnification X900.
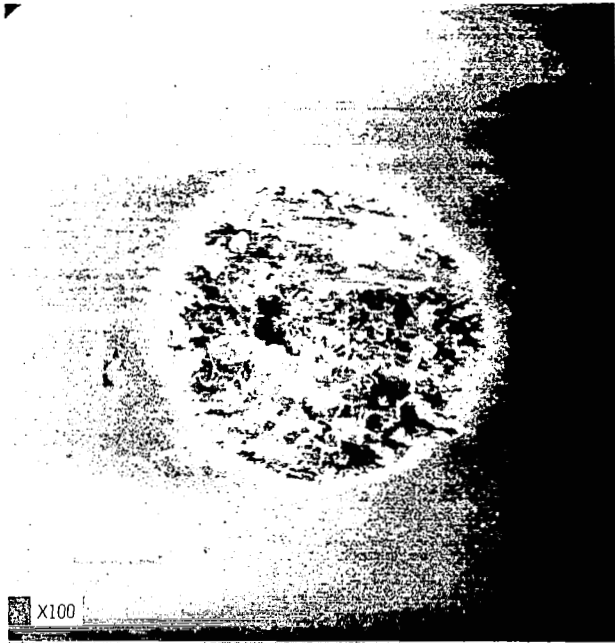

(c) Magnification, X3000.

Figure 14. – Scanning electron micrographs of Monel fretted against Monel for 10^3 cycles in air at room temperature. Frequency, 55.8 hertz; normal force, 1.47 newtons (150 g); amplitude, 75×10^{-6} meter. (Note what appears to be a transfer fragment (P) in (a) and (b).)

26
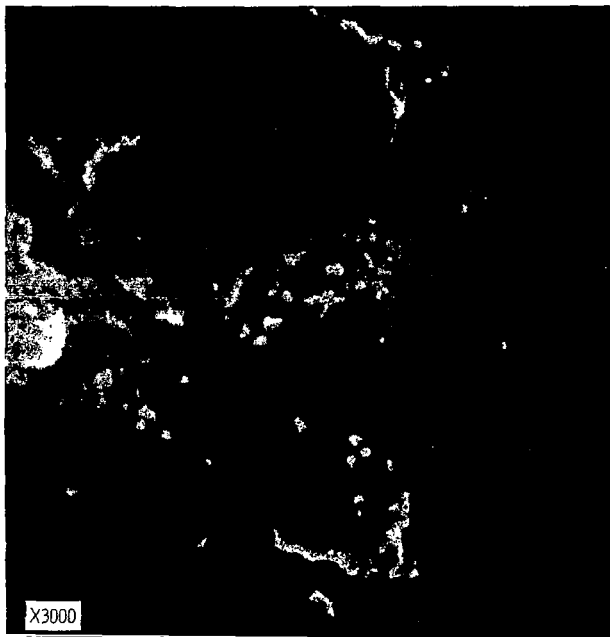
Figure 15. – Scanning electron micrographs of Monel fretted against Monel for 10^4 cycles in air at room temperature. Frequency, 55.8 hertz; normal force, 1.47 newtons (150 g); amplitude, 75×10^{-6} meter.
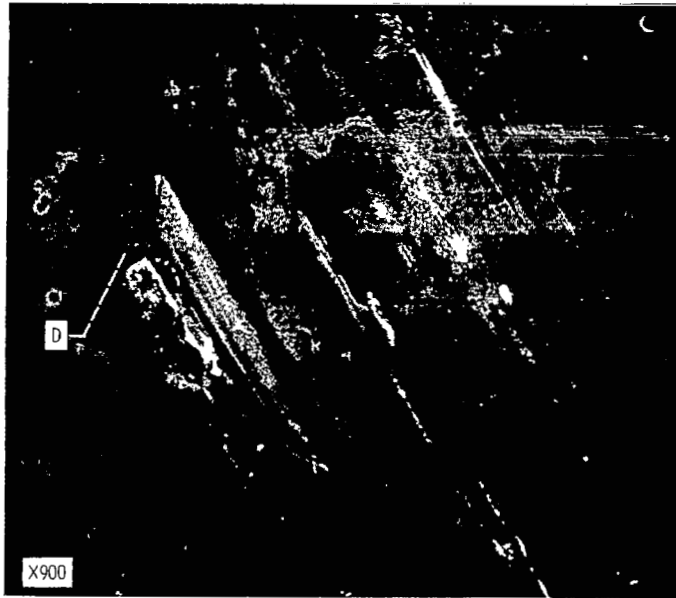
Figure 16. - Scanning electron micrographs of Monel fretted against Monel for 5x10^4 cycles in air at room temperature. Frequency, 55.8 hertz; normal force, 1.47 newtons (150 g); amplitude, 75x10^{-6} meter.

Figure 17. – Scanning electron micrographs of Monel fretted against Monel for 10^5 cycles in air at room temperature. Frequency, 55.8 hertz; normal force, 1.47 newtons (150 g); amplitude, 75×10^{-6} meter.
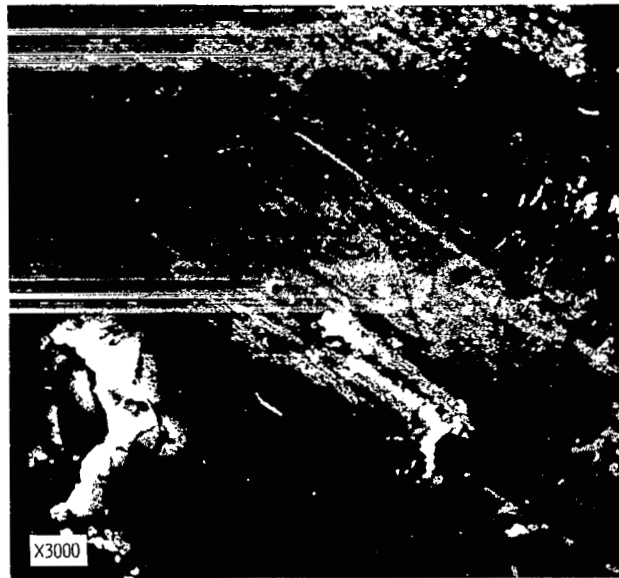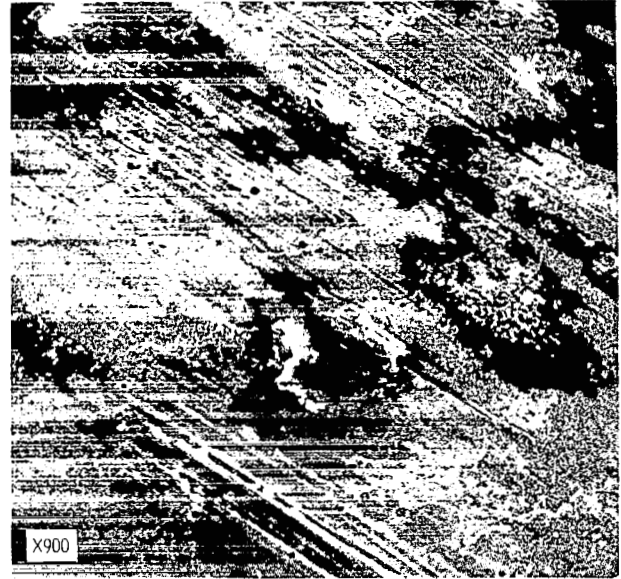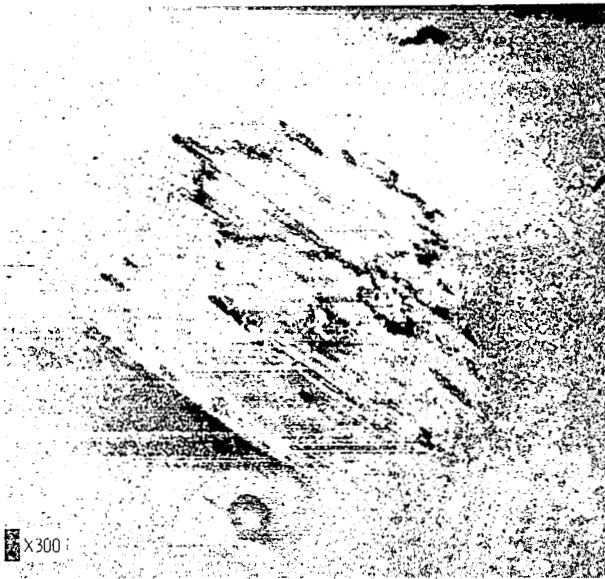
Figure 18. - Scanning electron micrograph of Co-25Mo fretted against Co-25Mo for 10^2 cycles in air at room temperature. Frequency, 55.8 hertz; normal force, 1.47 newtons (150 g); amplitude, 75×10^{-6} meter. (Note the debris (D) around the scratches.)
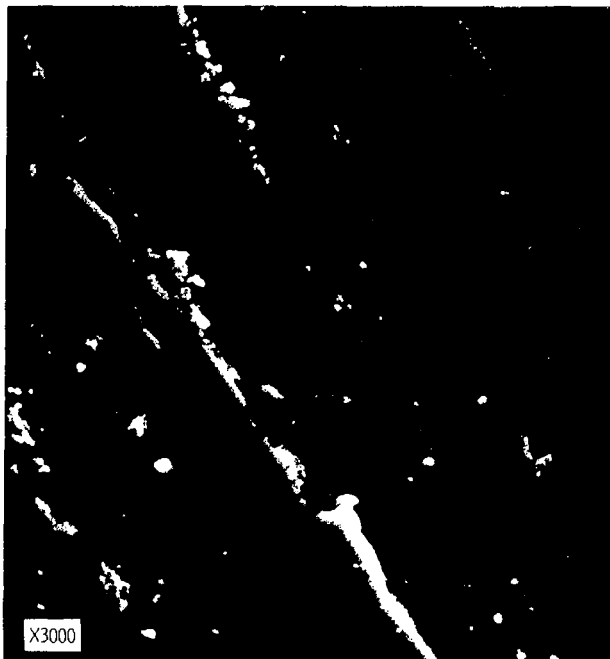
Figure 19. - Scanning electron micrographs of Co-25Mo fretted against Co-25Mo for 10^3 cycles in air at room temperature. Frequency, 55.8 hertz; normal force, 1.47 newtons (150 g); amplitude, 75×10^{-6} meter.
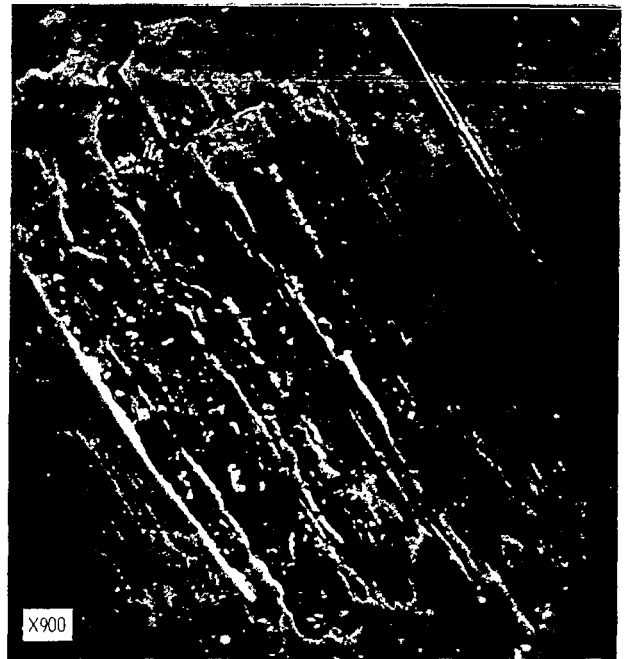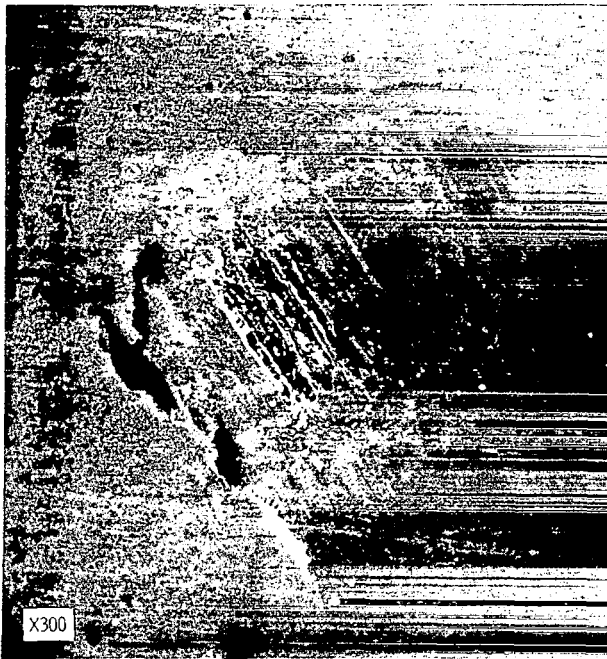
Figure 20. - Scanning electron micrographs of Co-25Mo fretted against Co-25Mo for 10^4 cycles in air at room temperature. Frequency, 55.8 hertz; normal force, 1.47 newtons (150 g); amplitude, 75×10^{-6} meter.

(a) Magnification, X200.

(b) Magnification, X900.

(c) Magnification, X3000.

Figure 21. - Scanning electron micrographs of Co-25Mo fretted against Co-25Mo for $2x10^5$ cycles in air at room temperature. Frequency, 55.8 hertz; normal force, 1.47 newtons (150 g); amplitude, $75x10^{-6}$ meter.
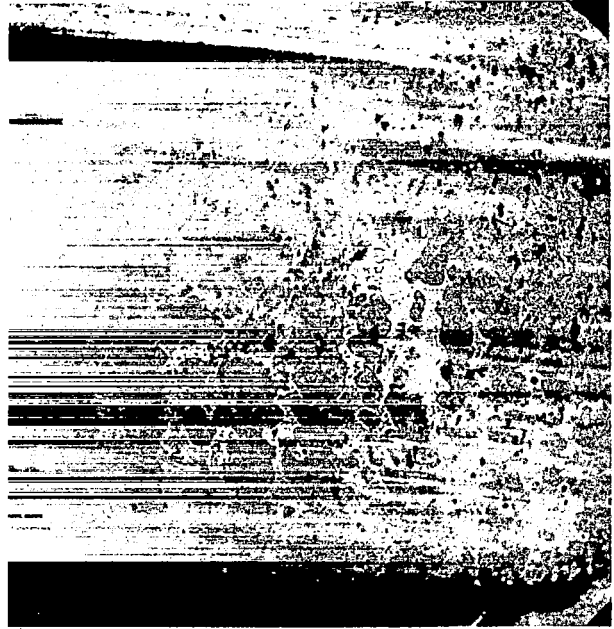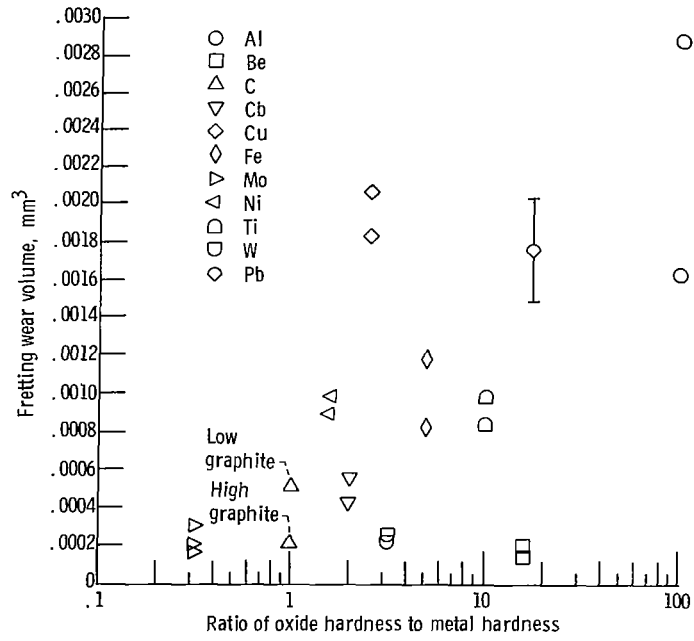
33

Fretting wear volume, mm^3

.0030
.0028
.0026
.0024
.0022
.0020
.0018
.0016
.0014
.0012
.0010
.0008
.0006
.0004
.0002
0

O   Al
□   Be
△   C
▽   Cb
◇   Cu
◊   Fe
▷   Mo
◁   Ni
⌂   Ti
�   W
◇   Pb

Low
graphite
High
graphite

.1   1   10   100

Ratio of oxide hardness to metal hardness

Figure 22. - Fretting wear volume after 6×10^5 cycles as function of ratio of oxide hardness to metal hardness.